the FEBS Journal

Use of 'small but smart' libraries to enhance the enantioselectivity of an esterase from *Bacillus stearothermophilus* towards tetrahydrofuran-3-yl acetate

Alberto Nobili*, Markus G. Gall*, Ioannis V. Pavlidis, Mark L. Thompson†, Marlen Schmidt and Uwe T. Bornscheuer

Department of Biotechnology and Enzyme Catalysis, Institute of Biochemistry, Greifswald University, Germany

Keywords
directed evolution; enantioselectivity; esterase; secondary alcohol; tetrahydrofuran-3-yl acetate

Correspondence
U. T. Bornscheuer, Department of Biotechnology and Enzyme Catalysis, Institute of Biochemistry, Greifswald University, Felix-Hausdorff-Str. 4, D-17487 Greifswald, Germany
Fax: +49 3834 86794367
Tel: +49 3834 864367
E-mail: uwe.bornscheuer@uni-greifswald.de
Website: http://biotech.uni-greifswald.de

†**Present address**
Manchester Institute of Biotechnology, School of Chemistry, The University of Manchester, 131 Princess Street, M1 7DN, UK

*These authors contributed equally to this work

(Received 19 November 2012, revised 8 January 2013, accepted 15 January 2013)

doi:10.1111/febs.12137

Two libraries of simultaneous double mutations in the active site region of an esterase from *Bacillus stearothermophilus* were constructed to improve the enantioselectivity in the hydrolysis of tetrahydrofuran-3-yl acetate. As screening of large mutant libraries is hampered by the necessity for GC/MS analysis, mutant libraries were designed according to a 'small but smart' concept. The design of focused libraries was based on data derived from a structural alignment of 3317 amino acid sequences of α/β-hydrolase fold enzymes with the bioinformatic tool 3DM. In this way, the number of mutants to be screened was substantially reduced as compared with a standard site-saturation mutagenesis approach. Whereas the wild-type esterase showed only poor enantioselectivity (E = 4.3) in the hydrolysis of (*S*)-tetrahydrofuran-3-yl acetate, the best variants obtained with this approach showed increased E-values of up to 10.4. Furthermore, some variants with inverted enantiopreference were found.

Introduction

Protein engineering has emerged as a scientific field that can improve the natural features of an enzyme to make industrial processes more feasible, paving the way through the three waves of biocatalysis [1,2]. In this context, several approaches have evolved to facilitate the discovery of mutants with beneficial catalytic properties, such as increased thermal or solvent stability [3,4] and enantioselectivity [5]. Among them, directed evolution is one of the most flexible and successful tools; however, one of its major drawbacks is that it

Abbreviations
BsteE, *Bacillus stearothermophilus* esterase; THF-3-Ac, tetrahydrofuran-3-yl acetate; THF-3-ol, tetrahydrofuran-3-ol.

relies on high-throughput screening, which is usually the bottleneck of this method [6,7]. In order to reduce the screening effort, more focused approaches were developed recently, including the use of a reduced amino acid alphabet. For instance, the NDT codon encodes only 12 amino acids, which represent all functional groups, and also the number of nonfunctional enzymes was reduced, as only one stop codon is encoded [5]. Moreover, experimental data showed that the beneficial mutations for the increases in enantioselectivity, substrate specificity and catalytic promiscuity are localized close to the catalytic active site, underlining the need for focused libraries [8].

In parallel with the development of these focused approaches, the amount of structural and catalytic information about enzymes from crystallography, genome sequencing and biochemical data has expanded dramatically during recent years, and new bioinformatics tools such as 3DM have been developed to make this wealth of information available to researchers [9,10]. The combination of bioinformatics with protein engineering has resulted in a set of more targeted approaches [10]. More sophisticated bioinformatics tools, such as structure-based alignment, elaborate biocatalytic data in a more consistent way, and the success rate of such approaches is significantly increased as compared with random approaches [9].

Enantiopure chiral compounds are frequently needed as building blocks in the pharmaceutical industry. For example, tetrahydrofuran-3-ol (THF-3-ol) is an important precursor for the production of HIV protease inhibitors [11,12]. Currently, there is no enzyme known that enantioselectively catalyses the production of THF-3-ol from tetrahydrofuran-3-yl acetate (THF-3-Ac) (Scheme 1), presumably because the substituents next to the chiral centre are highly similar. Until now, the production of optically pure THF-3-ol has been achieved either via chemical synthesis [11] or by enzymatic hydrolysis of bulkier esters and inversion of the unwanted product [13].

Herein, we present the enhancement of the enantioselectivity of an esterase from *Bacillus stearothermophilus*

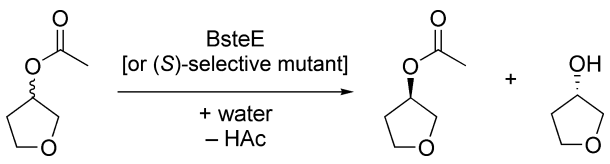

Scheme 1. (*R,S*)-THF-3-Ac enantioselective hydrolysis to (*S*)-THF-3-ol and acetic acid (HAc) catalysed by BsteE and the (*S*)-selective mutants.

(BsteE; EC 3.1.1.1) for the synthesis of the industrially interesting THF-3-ol from the corresponding acetate (THF-3-Ac), using 'small but smart' libraries [9]. BsteE was selected for this study because of the higher enantioselectivity shown in preliminary screening of hydrolases (data not shown). GC analysis was preferred to obtain accurate and reproducible results, despite the low throughput, as the coupled acetate assay [14] is not applicable, owing to the slow hydrolysis of THF-3-Ac (data not shown). The 'small but smart' approach, i.e. the use of data derived from the 3DM database to design the libraries, leads to a higher percentage of active mutants than site-saturation mutagenesis. This increases the possibility of obtaining a mutant with increased enantioselectivity, something that supports the use of such focused libraries as a shortcut to desired mutants.

Results

Construction of 'small but smart' libraries

In order to design mutant libraries of BsteE, target positions for the mutations first need to be defined. Three criteria were used for the identification of the target positions: (a) the amino acids should not actively participate in the catalytic mechanism – in this way, the catalytic triad and the residues of the loop of the oxyanion hole are excluded, as mutations at these positions would normally lead to loss of activity; (b) the positions should be in close vicinity to the substrate; and (c) the side chain should be oriented towards the substrate. The (*R*)- and (*S*)-enantiomer of THF-3-Ac were docked to the wild-type enzyme, and the results are presented in Fig. 1. Docking analysis revealed that the substrate interacts with the catalytic Ser94 and His223, but also with several other amino acids, which form a cavity for accommodation of the substrate. The most interesting positions for mutations are Asp31, Leu93, Met195 and Val224, which were selected for our study. Their side chains are < 3.5 Å away from the substrate, so they can interact upon mutation, but do not actively participate in the catalytic mechanism. Three of the selected positions are close to the catalytic triad (Ser94, His223, and Asp193), and, according to previous work [8], are capable of affecting the activity and selectivity of the enzyme. The substrate enantiomers also interact with amino acids at positions 23–27, but these amino acids are on a sharp turn, which forms the oxyanion hole, and are responsible for stabilization of the tetrahedral intermediate [15,16]. More specifically, the carboxylic oxygen of the substrate forms two hydrogen bonds with the backbone nitrogen atoms of

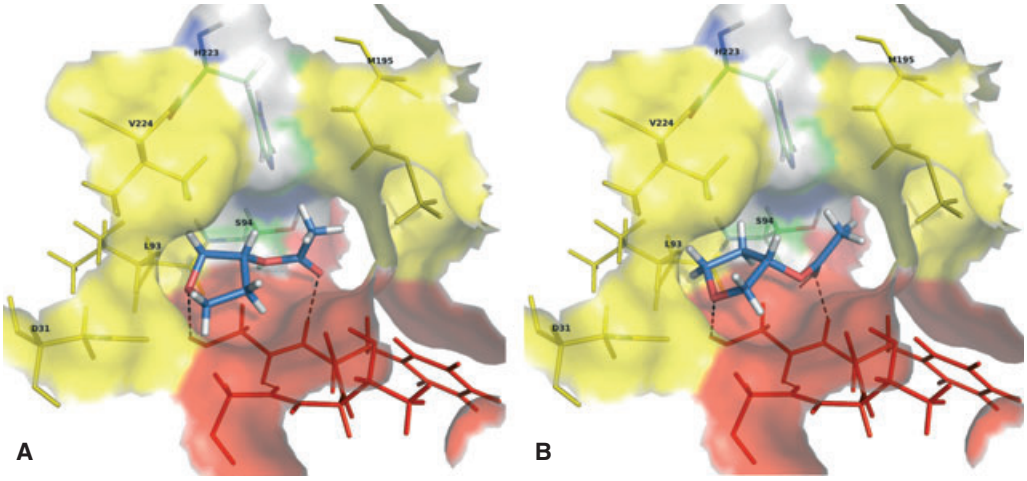

Fig. 1. (A) (*R*)-THF-3-Ac or (B) (*S*)-THF-3-Ac in the active site of wild-type BsteE, as predicted from the docking analysis. The catalytic Ser94 and His223 are presented with elemental colouring, the positions targeted for mutation are coloured yellow, and the amino acids of the loop that forms the oxyanionic hole are shown in red. The hydrogen bonds formed between the substrate and the enzyme and between Gly24 and Gly27 are denoted with dashes.

Phe25 and Leu95 (Fig. 1). The stabilization of the substrate in the active site by these two hydrogen bonds is in accordance with crystallographic data [17], verifying the results of the docking analysis. Moreover, Gly27 seems to stabilize the turn, as it forms a hydrogen bond with Gly24, which is located on the other branch of the loop. We were able to confirm that the G27D mutation negates any positive effect on the enantioselectivity resulting from the mutations at the other positions (data not shown).

On the basis of these results, we decided to prepare two libraries of double mutants: library I, with simultaneous mutations of Asp31 and Leu93; and library II, with Met195 and Val224 as targets. The distance of the target positions was taken into consideration in the coupling of the positions in the two libraries; the amino acids that are closer were combined in the same library, so any possible synergistic effects of simultaneous mutations could be observed.

The distribution of amino acids at these positions was determined by using the platform 3DM (http://www.bio-prodict.nl/), which builds protein superfamily-specific databases [18,19]. The structure-based alignment provided by the 3DM database ensures that the amino acids aligned are at equivalent structural positions. From the superfamily of α/β-hydrolase fold enzymes, we created a 3DM database with the sequences of hydrolase family VII (3317 sequences), of which BsteE is a member. As shown in Fig. 2, all four positions are quite variable, with the prevailing amino

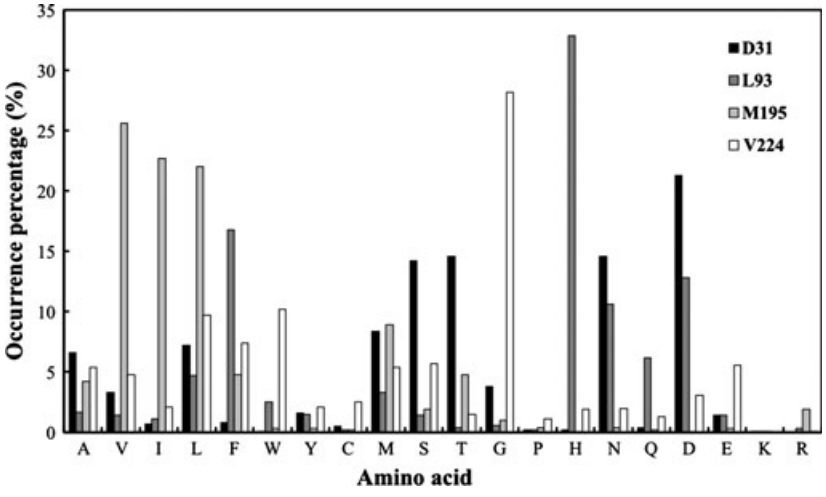

Fig. 2. Amino acid distribution within 3317 sequences for each position selected, as analysed from the 3DM database.

Table 1. Amino acids – predicted as allowed (occurrence: > 3%) – at four positions selected in BsteE according to the structure-based alignment from the 3DM database. In addition, the codons that were chosen for the design of the libraries and the corresponding amino acids are given.

Position	Allowed amino acids	Codon	Encoded amino acids
D31	A, D, G, L, M, N, S, T, V	RNY	A, D, G, I, N, S, T, V
L93	D, F, H, L, M, N, Q	DNK	A, C, D, E, F, G, I, K, L, M, N, R, S, T, V, W, Y
M195	A, F, I, L, M, T, V	DYK	A, F, I, L, M, S, T, V
V224	A, D, E, F, G, L, M, S, V, W	NWK	D, E, F, H, I, K, L, M, N, Q, V, Y

acid in all cases accounting for < 35%. Moreover, several amino acids occur frequently (more often than 3% among the aligned sequences). In previous work, it was shown that the naturally occurring amino acids seem to lead to correct folding of the protein and enzymatic activity, whereas the rareness of the other amino acids suggests that they have a negative effect on the protein activity [9]. In order to prepare 'small but smart' libraries, appropriate codons were designed to encode most of the frequently occurring amino acids (also denoted as allowed amino acids). Table 1 shows the allowed amino acids in all four selected positions, the codon used for each position, and the coded amino acids. The scale of the reduction of the screening effort can easily be calculated: if an NNK codon is used in a simultaneous double mutation library, a total of 3066 colonies need to be screened to achieve 95% library coverage [5]. Using the data derived from 3DM to design these libraries, we needed to screen only 1149 colonies for library I and 574 colonies for library II to achieve the same percentage of library coverage. It should be noted that the single mutants are also included in the libraries, as shown in Table 1. This significant decrease in the screening effort underlines the importance of the 3DM-based design of the libraries, especially if only low-throughput assays are available.

Screening of the libraries

Biocatalysis experiments were performed with all mutants and wild-type BsteE as a control. The enantioselectivity of the wild-type enzyme was calculated according to Chen *et al.* [20], and it was found to be slightly (*S*)-selective ($E = 4.3 \pm 0.2$). Most of the mutants in both libraries showed similar activity and enantioselectivity as the wild-type, justifying this way of using the 3DM database. Less than 3% of the mutants screened in library II showed conversion of < 5% after 42 h, whereas the average conversion for the whole library was 61%.

The most interesting mutants in terms of enantioselectivity that were found from the mutant libraries are shown in Table 2. As shown, replacement of Leu93 with phenylalanine had a positive effect on (*S*)-enantioselectivity only when a simultaneous mutation at position 31 occurred. Mutations at position 31 increased the (*S*)-enantiopreference up to $E = 6.0$ as single mutants, when small and less polar or nonpolar residues were used. However, the best mutant of library I was the D31T/L93F double mutant, with a 2.4-fold increase in the *E*-value. Detailed analysis of the corresponding single mutants revealed that the enhancement of enantioselectivity of the double mutant was attributable to synergistic effects, as both single mutants were found to be inferior. These observations confirm that it is important to design libraries with double mutations of amino acids in close vicinity, as the L93F single mutation would never be selected to further increase the (*S*)-enantioselectivity in a second round of mutation.

Table 2. Overview of the most interesting BsteE mutants and their respective *E*-values. The best mutants with enhanced (*S*)-selectivity from the two libraries were combined, and the results are presented in the lower part of the table. The mutants are sorted according to descending order of *E*-value for each subgroup.

Designation	Mutations	*E*-value
Wild-type	None	4.3 ± 0.2 (*S*)
Library I mutants	D31T/L93F	10.4 ± 0.1 (*S*)
	D31T	6.0 ± 0.1 (*S*)
	D31V	6.0 ± 0.4 (*S*)
	D31A	5.8 ± 0.0 (*S*)
	D31G/L93F	5.3 ± 0.3 (*S*)
	D31I/L93F	5.2 ± 0.1 (*S*)
	L93F	2.6 ± 0.0 (*S*)
Library II mutants	M195A	7.3 ± 0.2 (*S*)
	M195A/V224L	4.2 ± 0.0 (*S*)
	M195T	3.8 ± 0.2 (*S*)
	M195T/V224Y	1.4 ± 0.0 (*R*)
	V224Y	1.4 ± 0.0 (*R*)
Combinations	D31T/L93F/M195A	10.3 ± 0.3 (*S*)
	D31G/L93F/M195A	6.3 ± 0.2 (*S*)
	D31V/M195A	6.7 ± 0.2 (*S*)

The results of library II screening revealed lower enhancement of the (*S*)-enantiopreference. The best mutant, M195A, showed a 1.7-fold increase in enanti-

oselectivity. No other interesting mutants were observed in this library, and the simultaneous mutation with position 224 destroyed any positive effect of the M195A mutation. For example the V224L mutation negated any positive effect that the M195A mutation had, although it is still a hydrophobic nonpolar residue. It seems that positions 195 and 224 cannot have synergistic effects, because the catalytic histidine lies between these two amino acids (Fig. 1). The most interesting finding, however, is that position 224 seems to be responsible for the inversion of enantioselectivity. A few mutants showed marginal (*R*)-enantiopreference in this library, whereas no mutants with such selectivity were observed in library I. It seems that the V224Y mutation is responsible for the inversion of enantioselectivity, as the single mutant and the double mutant M195T/V224Y showed similar profiles. Although the *E*-value is low, the V224Y mutant could be used as a starting point for a further mutation round in order to prepare an (*R*)-selective esterase.

Targeting further improvement of (*S*)-selectivity, we combined the M195A mutation – which proved to be the only interesting (*S*)-selective mutation in library II – with some of the best mutants from library I, in order to evaluate any possible synergistic effects. As can be seen in Table 2, there was no additive effect when the M195A mutation was incorporated into the best mutants of library I. In the case of the D31G/L93F and D31V mutants, where the *E*-value was lower than of the single mutant M195A, a slight increase could be observed when the latter mutation was added. For the best mutant, D31T/L93F, no effect was observed. An explanation for this phenomenon may be the available space provided to the substrate in order for it to approach the catalytic serine. Positions 31 and 195 are on opposite sides of the long axis of the docked substrate, as shown in Fig. 1. As discussed previously, in order to increase the (*S*)-enantiopreference of BsteE, smaller and less polar or nonpolar amino acids are required in these positions. Therefore, as the side chains are not interacting with the substrate any more, these mutations would provide greater space and subsequently more freedom for the substrate to approach Ser94. It seems that a crucial amount of space is needed in this axis, in order to overcome any steric hindrance that other side chains produce from other directions, and is responsible for the enantioselectivity of this enzyme. This is in line with previous work showing that the substitution of bulky residues that form the bottleneck to the active site with smaller ones results in substantially increased enantioselectivity [21,22]. However, if both mutations occur simultaneously, the effect is not additive, as the provision of more space and freedom does not have any further effect. This is not the case for the D31T/L93F mutant, as the threonine at position 31 interacts with the substrate.

Discussion

Screening of the two 'small but smart' libraries of double mutants led to a 2.4-fold increase in the (*S*)-enantioselectivity of BsteE towards THF-3-Ac, through implementation of the D31T/L93F mutations. Despite the fact that the obtained *E*-value of 10.4 leaves room for further improvement, the achieved enhancement of enantioselectivity towards this racemic substrate with substituents of high similarity with the use of these focused libraries is a major achievement as compared with previous work of a similar nature. Four consecutive rounds of random mutagenesis by error-prone PCR and screening of 7600 clones led to a *Pseudomonas aeruginosa* PAO1 lipase mutant with an *E*-value of 11.3 for a much easier substrate to resolve – in terms of substituents – such as *p*-nitrophenyl 2-methyldecanoate [23]. In a more focused approach, saturation mutagenesis at certain positions of *Pseudomonas fluorescens* esterase increased the *E*-value from 3.5 to 12 for ethyl 3-phenylbutanoate [24]. These results also support the use of 'small but smart' libraries as a fast approach to obtain the desired mutants with less screening effort. In order to underline the difficulty of THF-3-Ac kinetic resolution, owing to its similar substituents, it should be mentioned that, after screening of several commercially available hydrolases for the kinetic resolution of a similar substrate, such as 3-hydroxycyclopentanone, by transesterification with vinyl acetate, the best hydrolase was revealed to be an immobilized esterase with an *E*-value of 11 [25].

Docking calculations were performed with both enantiomers of the ester, and the tetrahedral intermediate was prepared in order to obtain an insight into the enantioselectivity mechanism. The enantiomers were docked into the wild-type esterase, the V224Y mutant, which has low (*R*)-enantioselectivity, and the D31T/L93F double mutant [the best (*S*)-selective mutant identified]. The tetrahedral intermediate is stabilized in most cases by the formation of two hydrogen bonds between the oxyanion and the Phe25 and the Leu95 backbone nitrogen atoms. This is in line with crystallographic data, and confirms the accuracy of our docking analysis [17].

As described above, wild-type BsteE shows low (*S*)-enantiopreference. The reason for this catalytic behaviour lies in the stabilization of the tetrahedral intermediate through a hydrogen bond network [26]. As

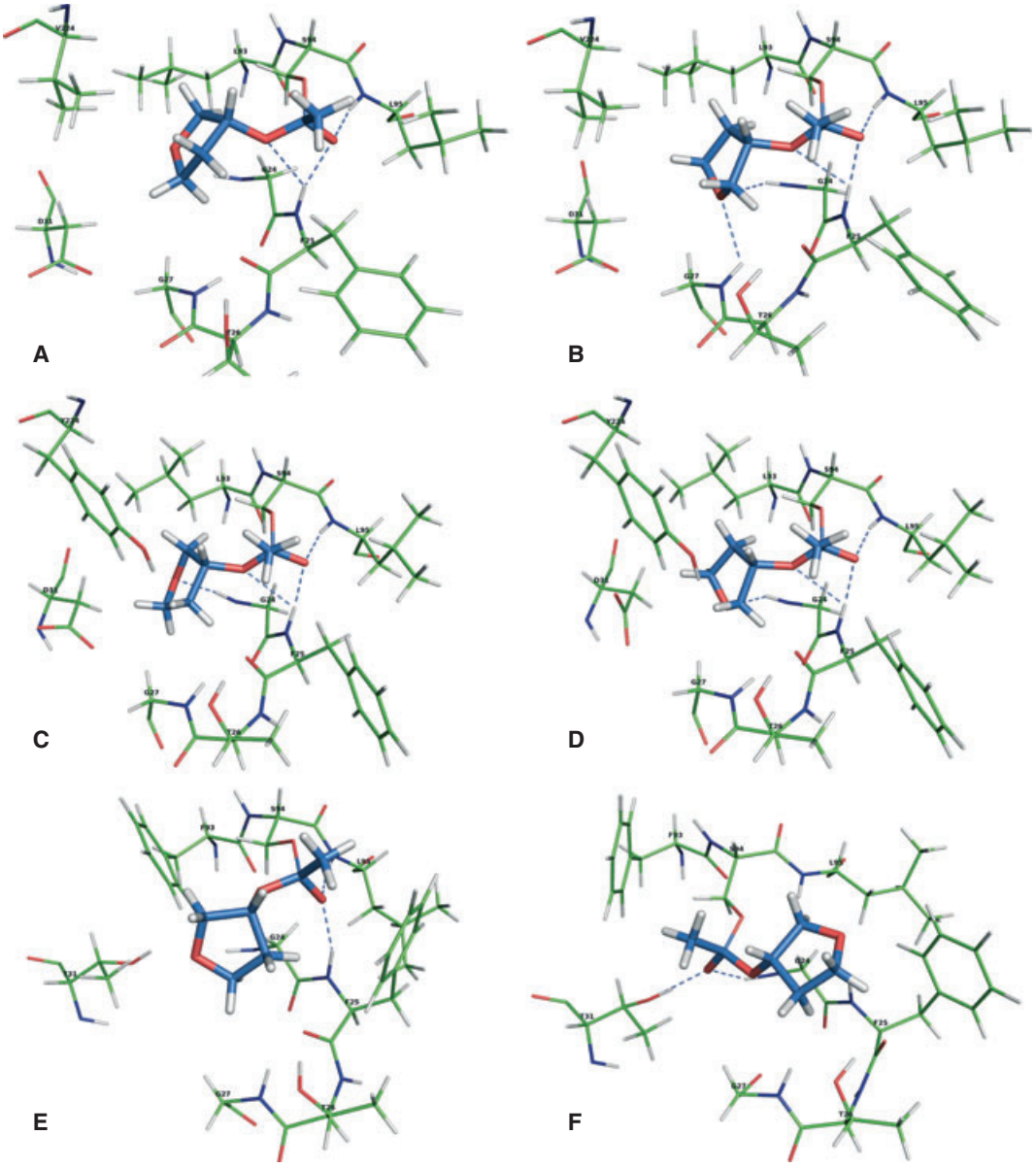

Fig. 3. Energy-minimized tetrahedral intermediates of wild-type BsteE (A, B) and the V224Y (C, D) and D31T/L93F (E, F) mutants with both enantiomers of the ester [(A, C, E) (*R*)-THF-3-Ac; (B, D, F) (*S*)-THF-3-Ac]. The hydrogen bonds formed between the substrate and the protein are denoted with dashes.

shown in Fig. 3B, the (*S*)-THF-3-Ac tetrahedral intermediate is stabilized by five hydrogen bonds: three to the oxyanion and ester oxygen, and two to the oxygen of the furan ring from Gly24 and Gly27. In the case of (*R*)-THF-3-Ac (Fig. 3A), the latter two hydrogen bonds are not present, and thus the furan ring is more flexible than in the (*S*)-enantiomer; an effect that reduces the reactivity of this enantiomer. This stabilization leads to a more catalytically active conformation of the (*S*)-ester in a molecular dynamic simulation than those predicted for the (*R*)-enantiomer (56.9% and 32.8%, respectively).

In the case of the V224Y mutant with inverted selectivity, the tyrosine that is inserted at position 224 is oriented towards the loop that forms the oxyanion hole. The presence of this bulky group instead of valine forces the furan ring to move closer to one branch of the loop, as observed in Fig. 3C,D. The consequence of this is that the backbone nitrogen from Gly24 forms a hydrogen bond with the oxygen from the furan ring in

both enantiomers. The difference that the two tetrahedral intermediates had in the wild-type is eliminated, and both docked structures appear to be almost identical. The low (*R*)-preference that is also shown by molecular dynamic experiments [catalytically active conformations: 32.0% for (*R*)-THF-3-Ac, and 31.1% for (*S*)-THF-3-Ac] seems to result from the shorter hydrogen bond (and thus stronger interaction) between Gly24 and the furan oxygen of the (*R*)-enantiomer.

The D31T/L93F double mutant showed the best (*S*)-enantiopreference among the mutants screened. As shown in Fig. 3E,F, the phenylalanine at position 93 forces the furan ring to move away from the oxyanion hole, and thus destabilizes the tetrahedral intermediate. According to the docking results, the (*R*)-enantiomer binds in a similar way to the wild-type enzyme (Fig. 3E), with the oxyanion forming two hydrogen bonds with Phe25 and Leu95, as in all previous cases. However, the furan ring is pushed away from the oxyanion hole by Phe93, so the ester oxygen atom can no longer form the hydrogen bond with Phe25, and the flexibility of this enantiomer therefore increases. On the other hand, the (*S*)-enantiomer binds to the catalytic serine in the opposite orientation (Fig. 3F), a structure that is not predicted from the crystallographic data [17]. The acetate group is positioned towards Phe93, and the furan ring is directed towards a more open space. Both mutations seem to contribute to the inversion of the (*S*)-ester orientation; the bulky phenylalanine at position 93 causes steric hindrance to the positioning of the ring over Gly24, whereas the simultaneous Thr31 mutation stabilizes the tetrahedral intermediate by hydrogen bonding to the oxyanion. The intrinsic reason why the inverted positioning is favoured is not fully understood, as both enantiomers form only two hydrogen bonds with their oxyanions. However, it seems that (*S*)-THF-3-Ac is favoured, as it does not suffer from the steric hindrance of Phe93, whereas (*R*)-THF-3-Ac needs to bind in a strictly confined area with a very specific orientation. This seems to agree with the molecular dynamic results; no catalytically active structures are predicted for the inversed orientation of (*S*)-THF-3-Ac. This provides an insight into the mechanism of selectivity; the enantiopreference does not rely on the stabilization of the tetrahedral intermediate (as in the previous cases), but possibly on the binding of the substrate and the formation of the tetrahedral intermediate; as steric hindrance prevents the (*R*)-enantiomer from binding to the active site, (*S*)-selectivity will be observed, even if the new (inverted) conformation is not as catalytically active as the one observed for the wild-type. The reversed orientation of the (*S*)-enantiomer in this double mutant could be a good starting point for another round of mutations to further increase the enantioselectivity.

In conclusion, the use of these 'small but smart' libraries significantly facilitated the enhancement of BsteE's (*S*)-enantioselectivity towards a substrate with similar substituents, by 2.4-fold, and led to a substantial reduction in the screening effort; and the *in silico* analysis provided insights into the mechanism of the enantioselectivity.

Experimental procedures

General

All chemicals were purchased from Fluka (Buchs, Switzerland), Sigma (Steinheim, Germany), and Merck (Darmstadt, Germany), unless stated otherwise. Primers were synthesized by Invitrogen (Darmstadt, Germany), and the sequencing was performed by GATC Biotech (Konstanz, Germany).

Chemical synthesis of THF-3-Ac

Racemic THF-3-Ac was prepared with described previously published methods [27]. Acetyl chloride (40 mmol) was dissolved in 20 mL of pyridine at 4 °C, and the mixture was stirred thoroughly before a solution of THF-3-ol (40 mmol) in CH_2Cl_2 (25 mL) was added slowly to the mixture. The mixture was kept at 4 °C without stirring for 30 min, and was then stirred at room temperature for 28 h. The mixture was diluted with ether (200 mL), washed with $NaHCO_3$ (saturated aqueous solution, 3 × 200 mL), the aqueous phase was extracted with ether (3 × 200 mL), and all organic phases were combined and dried over anhydrous Na_2SO_4. The solvent was then removed *in vacuo*, before purification by vacuum distillation (boiling point of 95 °C at 97 mbar) to give the ester as a colourless oil (5.08 g, 39 mmol, 97.6% yield).

^{1}H-NMR (300 MHz, $CDCl_3$): 5.29 (1H, m, 3-H), 4.03–3.73 (4H, m, 2-H_2 and 5-H_2), and 2.28–1.85 (5H, m, 4-H_2 and 3-$COCH_3$).

^{13}C-NMR (75 MHz, $CDCl_3$): 170.9, 74.9, 73.1, 66.9, 32.7, and 21.18.

Construction of the library

Both libraries were constructed by two subsequent QuikChange reactions. The following reaction mixture was prepared: distilled H_2O (35.0 μL), 10 × Pfu Plus! Buffer (5.0 μL), dNTPs (1.0 μL, 10 mM each), plasmid pGASTON containing the gene encoding BsteE (2.0 μL, 10 ng·μL^{-1}), forward primer (1.5 μL, 10 μM), reverse primer (1.5 μL, 10 μM), dimethylsulfoxide (3.0 μL), and Pfu Plus! DNA Polymerase (1.0 μL, 5 U·μL^{-1}). The reaction was performed with the

following thermocycling conditions: one cycle of 95 °C for 300 s; 18 cycles of 95 °C for 60 s, 50/55/60/65 °C for 60 s, and 75 °C for 230 s; and one cycle of 72 °C for 600 s. Then, *Dpn*I (1 μL) was added, and the samples were incubated for 1 h at 37 °C; this was followed by enzyme denaturation for 10 min at 80 °C. Chemocompetent *Escherichia coli* cells (DH5α) were transformed with the amplified plasmid (4 μL) and plated out on LB_{AMP} plates. The transformed cells were grown on agar plates at 37 °C until an appropriate size was achieved, and then picked, placed in microtiter plates containing LB_{AMP} medium, and incubated overnight at 37 °C. On the following day, glycerol stocks were prepared from these microtiter plates, and kept at −80 °C until screening. The success of the library creation was confirmed by sequencing of several randomly picked mutants.

Primers

Library I

D31-RNY-FW, 5′-GTTTACCGGCAATTCCGCTRNYGTTCGGATGC-3′; D31-RNY-RV, 5′-GCATCCGAACRNYAGCGGAATTGCCGGTAAAC-3′; L93-DNK-FW, 5′-CGCCGTCGCCGGADNKTCGCTTGGAGG-3′; and L93-DNK-RV, 5′-CCTCCAAGCGAMNHTCCGGCGACGGCG-3′.

Library II

M195-DYK-FW, 5′-CAGGCGCGCCATGATGAGDYKATCAACCCG-3′; M195-DYK-RV, 5′-CGGGTTGATMRHCTCATCATGGCGCGCCTG-3′; V224-NWK-FW, 5′-GCAATCAGGCCATNWKATTACGCTTGATC-3′; and V224-NWK-RV, 5′-GATCAAGCGTAATMWNATGGCCTGATTGC-3′.

Single mutations

D31T-FW, 5′-GCAATTCCGCTACCGTTCGGATGC-3′; D31T-RV, 5′-GCATCCGAACGGTAGCGGAATTGC-3′; L93F-FW, 5′-CGCCGGATTTTCGCTTGGAG-3′; L93F-RV, 5′-CCAAGCGAAAATCCGGCGAC-3′; M195A-FW, 5′-CCATGATGAGGCGATCAACCCGGACAGC-3′; M195A-RV, 5′-GCTGTCCGGGTTGATCGCCTCATCATGG-3′; M195T-FW, 5′-CCATGATGAGACCATCAACCCGGACAGC-3′; M195T-RV, 5′-GCTGTCCGGGTTGATGGTCTCATCATGG-3′; V224Y-FW, 5′-GCAATCAGGCCATTATATTACGCTTGATC-3′; and V224Y-RV, 5′-GATCAAGCGTAATATAATGGCCTGATTGC-3′.

Bacterial strains, growth conditions, and protein analysis

The vector pGASTON with a rhamnose-inducible promoter was used for the expression of BsteE and subsequent mutants [28]. All variants were expressed in *E. coli* DH5α at 30 °C. To screen the libraries, the cultivation was carried out in deep-well blocks. TB medium was inoculated with an overnight culture of the respective variant, and the induction was performed by addition of rhamnose (final concentration: 0.02%, v/v) 4 h later. Twenty hours after induction, the cells were harvested by centrifugation (6000 ***g***, 15 min, 4 °C). The pellet was washed with phosphate buffer (50 mM, pH 7.5), and cells were disrupted with BugBuster Protein Extraction Reagent (Merck). The cell debris was removed by another centrifugation step (6000 ***g***, 15 min, 4 °C), and the supernatant was transferred to a new microtiter plate and stored at 4 °C until use. For the interesting clones, larger-scale cultivations were performed (30 mL) with the same procedure, except that the cell disruption was performed by sonication on ice (5 min, 50% pulse, 50% power) after the pellet had been resuspended in phosphate buffer (50 mM, pH 7.5). Soluble expression was confirmed by SDS/PAGE (data not shown).

Biocatalysis conditions and chiral GC/MS analysis

THF-3-Ac (12.5 mM) was added to the crude extract to start the reaction. Biocatalysis was carried out at 37 °C and 800 r.p.m. in a thermoshaker. Aliquots (200 μL) were removed at standard time intervals for a period of 42 h. The aliquots (200 μL) were extracted with 500 μL of CH_2Cl_2, and dried over $NaSO_4$. The analysis of all reactants is not possible with one column, so different columns were used to determine the enantiomeric excess of substrate and product. All samples were analysed at least in triplicate.

Analysis of substrates on a Hydrodex-*β*-3P column (Macherey-Nagel)

The column flow rate was 1.9 $mL \cdot min^{-1}$ of helium, and the reactants were eluted with an isothermal program at 70 °C (12 min). The retention times for the reactants were as follows: (*R,S*)-THF-3-ol, 7.9 min; (*R*)-THF-3-Ac, 8.7 min; and (*S*)-THF-3-Ac, 10.3 min.

Analysis of products on a Hydrodex-*β*-TBDAc column (Macherey-Nagel)

The column flow rate was 1.9 $mL \cdot min^{-1}$ of helium, and the reactants were eluted with the following program: 18 min at 110 °C, heating up to 180 °C at 15 $°C \cdot min^{-1}$, and holding at this temperature for 5 min. In this case, the retention times were as follows: (*S*)-THF-3-ol, 14.8 min; and (*R*)-THF-3-ol, 16.6 min.

Enantioselectivity values (*E*) and conversion were calculated with the formulae derived by Chen *et al.* [20]. All *E*-values were calculated at ~ 50% conversion.

In silico analysis of substrate docking

The substrate docking was performed with YASARA 11.11.2, and the figures were prepared with PYMOL 1.2. The crystal structure of BsteE (Protein Data Bank ID: 1TQH) was refined, and this structure was used for further *in silico* experiments. The AMBER03 force field was applied for substrate energy minimization and substrate docking. In order to compare the wild-type esterase with the best mutants, we prepared the tetrahedral intermediate, energy minimized, and superposed the structures. For the molecular dynamics experiment, the tetrahedral intermediate was used to evaluate the percentage of catalytically active structures. For this experiment, AMBER03 was used as a force field, and the experiment was run for 2 ns, with snapshots being taken every 25 fs in the biocatalysis conditions (37 °C, pH 7.5). As catalytically active conformations, the snapshots that could form viable hydrogen bond network (in terms of distance and angle) at the catalytically active triad and the oxyanion of the substrate were evaluated.

Acknowledgements

This project is part of the European Research Training Network on Directed Evolution of Functional Proteins (ENEFP, grant number 215560), funded by Marie-Curie Actions. We would like to thank A. Gollin for her help with the chemical synthesis.

References

1 Bornscheuer UT, Huisman GW, Kazlauskas RJ, Lutz S, Moore JC & Robins K (2012) Engineering the third wave of biocatalysis. *Nature* **485**, 185–194.
2 Lutz S & Bornscheuer UT (2008) Protein Engineering Handbook, Vols **1** and **2**, 1st edn. Wiley-VCH Verlag, Weinheim, Germany.
3 O'Fágáin C (2011) Engineering protein stability. *Methods Mol Biol (Clifton NJ)* **681**, 103–136.
4 Doukyu N & Ogino H (2010) Organic solvent-tolerant enzymes. *Biochem Eng J* **48**, 270–282.
5 Reetz MT (2011) Laboratory evolution of stereoselective enzymes: a prolific source of catalysts for asymmetric reactions. *Angew Chem Int Ed* **50**, 138–174.
6 Gupta RD & Tawfik DS (2008) Directed enzyme evolution via small and effective neutral drift libraries. *Nat Methods* **5**, 939–942.
7 Reymond JL (ed.) (2006) Enzyme Assays: High-Throughput Screening, Genetic Selection and Fingerprinting. Wiley-VCH, Weinheim.
8 Morley KL & Kazlauskas RJ (2005) Improving enzyme properties: when are closer mutations better? *Trends Biotechnol* **23**, 231–237.
9 Jochens H & Bornscheuer UT (2010) Natural diversity to guide focused directed evolution. *ChemBioChem* **11**, 1861–1866.
10 Gustafsson C, Govindarajan S & Minshull J (2003) Putting engineering back into protein engineering: bioinformatic approaches to catalyst design. *Curr Opin Biotechnol* **14**, 366–370.
11 Gadakh SK, Santhosh Reddy R & Sudalai A (2012) Enantioselective synthesis of HIV protease inhibitor amprenavir via co-catalyzed HKR of 2-(1-azido-2-phenylethyl)oxirane. *Tetrahedron Asymmetry* **23**, 898–903.
12 Honda Y, Katayama S, Kojima M, Suzuki T, Kishibata N & Izawa K (2004) New approaches to the industrial synthesis of HIV protease inhibitors. *Org Biomol Chem* **2**, 2061–2070.
13 Nomoto F, Shirasaka N & Otsuka K (1998) Production of optically active 3-hydroxytetrahydrofuran, Japanese Patent Application No. JP10337197A.
14 Baumann M, Stürmer R & Bornscheuer UT (2001) A high-throughput-screening method for the identification of active and enantioselective hydrolases. *Angew Chem Int Ed* **40**, 4201–4204.
15 Mandrich L, Menchise V, Alterio V, De Simone G, Pedone C, Rossi M & Manco G (2008) Functional and structural features of the oxyanion hole in a thermophilic esterase from *Alicyclobacillus acidocaldarius*. *Proteins Struct Funct Bioinf* **71**, 1721–1731.
16 Gall M, Kourist R, Schmidt M & Bornscheuer UT (2010) The role of the GGGX motif in determining the activity and enantioselectivity of pig liver esterase towards tertiary alcohols. *Biocatal Biotransform* **28**, 201–208.
17 Liu P, Wang Y-F, Ewis HE, Abdelal AT, Lu C-D, Harrison RW & Weber IT (2004) Covalent reaction intermediate revealed in crystal structure of the *Geobacillus stearothermophilus* carboxylesterase Est30. *J Mol Biol* **342**, 551–561.
18 Kourist R, Jochens H, Bartsch S, Kuipers R, Padhi SK, Gall M, Böttcher D, Joosten HJ & Bornscheuer UT (2010) The α/β-hydrolase fold 3DM database (ABHDB) as a tool for protein engineering. *ChemBioChem* **11**, 1635–1643.
19 Kuipers RK, Joosten HJ, van Berkel WJH, Leferink NGH, Rooijen E, Ittmann E, van Zimmeren F, Jochens H, Bornscheuer U, Vriend G *et al.* (2010) 3DM: systematic analysis of heterogeneous superfamily data to discover protein functionalities. *Proteins Struct Funct Bioinf* **78**, 2101–2113.
20 Chen CS, Fujimoto Y, Girdaukas G & Sih CJ (1982) Quantitative analyses of biochemical kinetic resolutions of enantiomers. *J Am Chem Soc* **104**, 7294–7299.
21 Schließmann A, Hidalgo A, Berenguer J & Bornscheuer UT (2009) Increased enantioselectivity by engineering bottleneck mutants in an esterase from *Pseudomonas fluorescens*. *ChemBioChem* **10**, 2920–2923.

22 Hidalgo A, Schließmann A, Molina R, Hermoso J & Bornscheuer UT (2008) A one-pot, simple methodology for cassette randomisation and recombination for focused directed evolution. *Prot Eng Des Sel* **21**, 567–576.
23 Reetz MT, Zonta A, Schimossek K, Liebeton K & Jaeger K-E (1997) Creation of enantioselective biocatalysts for organic chemistry by *in vitro* evolution. *Angew Chem Int Ed* **36**, 2830–2832.
24 Horsman GP, Liu AMF, Henke E, Bornscheuer UT & Kazlauskas RJ (2003) Mutations in distant residues moderately increase the enantioselectivity of *Pseudomonas fluorescens* esterase towards methyl 3-bromo-2-methylpropanoate and ethyl 3-phenylbutyrate. *Chem Eur J* **9**, 1933–1939.
25 Chen B-S & Hanefeld U (2013) Enantioselective preparation of (*R*) and (*S*)-hydroxycyclopentanone resolution. *J Mol Catal B Enzym* **85–86**, 239–242.
26 Ottosson J, Fransson L & Hult K (2002) Substrate entropy in enzyme enantioselectivity: an experimental and molecular modeling study of a lipase. *Protein Sci* **11**, 1462–1471.
27 Baumann M, Hauer BH & Bornscheuer UT (2000) Rapid screening of hydrolases for the enantioselective conversion of 'difficult-to-resolve' substrates. *Tetrahedron: Asymmetry* **11**, 4781–4790.
28 Henke E & Bornscheuer UT (2003) Esterases from *Bacillus subtilis* and *B. stearothermophilus* share high sequence homology but differ substantially in their properties. *Appl Microbiol Biotechnol* **60**, 320–326.